

Dwy

## RESISTIVITY MONITORING OF FLUID MIGRATION AT THE CERRO PRIETO GEOTHERMAL FIELD

N.E. Goldstein, K. Pruess, M.J. Wilt, and G.S. Bodvarsson

Earth Sciences Division  
Lawrence Berkeley Laboratory, University of California  
Berkeley, California 94720

### ABSTRACT

Apparent resistivities, measured by means of repetitive, dipole-dipole dc resistivity surveys since 1979, show significant and somewhat systematic changes over the area of the Cerro Prieto "a" reservoir. These changes are attributed to temperature and salinity changes, consequences of production, and natural recharge. To better understand the observed geophysical phenomena, we performed a series of simple reservoir simulation studies combined with the appropriate dc resistivity calculations to determine the magnitude and form of resistivity change. We considered production from a liquid-dominated reservoir with dimensions and parameters of the Cerro Prieto a reservoir and assumed lateral and vertical recharge of colder, less saline waters. The associated apparent resistivities increase 10 to 20% over the production area during a 3 year period at the current rate of production. These calculated changes agree in magnitude with the observed changes for the same production period. However, displayed in conventional pseudosection form, the patterns of calculated resistivity change only partially resemble the observed data. This is explained by the fact that natural recharge into the a reservoir is more complicated than our simple two-dimensional schematic recharge model. It is concluded that if properly conducted, dc resistivity monitoring appears capable of providing indirect information on fluid flow processes, including reinjection in a producing reservoir. Such information is extremely valuable for the development of quantitative predictions of reservoir performance.

### INTRODUCTION

Since the inception of the joint U.S. Department of Energy (DOE) - Comision Federal de Electricidad (CFE) reservoir engineering project to study the Cerro Prieto Geothermal Field, LBL and CFE have conducted numerous dc resistivity surveys to help define the reservoir and map subsurface structures and thermal conditions. Beginning in 1978, we have undertaken repetitive resistivity measurements along one long line that passes directly over the producing reservoir on the assumption that reservoir parameters altered by production might be indi-

rectly monitored from the surface. This technique was suggested by Risk's studies at the Broadlands Geothermal Field (Risk, 1975). Recently, similar investigations have also been extended to monitoring formation resistivity changes accompanying tertiary oil recovery (Bartel and Wayland, 1981).

Since 1979, when we were satisfied our field technique produced high quality data, we have observed rather systematic changes in apparent resistivities that could be caused by several possible hydrological, thermophysical and thermochemical mechanisms (Wilt and Goldstein, 1981a, 1981b). (i) natural recharge of less saline ground waters, (ii) coalescence of two-phase zones near the wells into a more extensive two-phase region, (iii) gradual cooling, and (iv) porosity reduction due to the precipitation of zeolites and carbonates as cooler waters react with the hotter rocks near the reservoir boundaries.

When the apparent resistivity changes were first noticed, we attempted to explain them using simple conjectured resistivity models (Wilt and Goldstein, 1981a). The results were unconvincing, and we therefore studied the problem in a more rigorous fashion. First we applied numerical modeling techniques to map the migration of waters of different temperature and salinity in response to production. Next we used computed changes of temperature and salinity within volume elements of the numerical model to estimate changes in apparent resistivity that would be observed at the surface. Although our studies employ rather schematic and simplified reservoir models, they demonstrate the technique of combining reservoir engineering and geophysical methods for reservoir monitoring.

### RESISTIVITY CHANGES OVER THE RESERVOIR

Figure 1 shows in pseudosection form the magnitude and pattern of resistivity change relative to baseline data collected in the Fall of 1979. The field data were collected using the dipole-dipole array with a dipole length of 1.0 km and dipole separations  $n$  from 1 to 8 ( $n$  = integer multiples of the dipole length). Results are plotted at the intersection of the 45° diagonals subtended from the mid-points of the

transmitter and receiver dipoles. In these pseudosections the  $n$ -spacing bears a rough relationship to depth of exploration. For example, at  $n=1$  most of the information comes from the upper 600 m, whereas at  $n=8$  most of the information is a volume averaged composite of the upper 2 km. The  $\alpha$  production zone lies approximately between resistivity electrodes 10 and 12 at a depth of 1.1 to 1.4 km. However, as lateral discontinuities in resistivity manifest themselves as diagonal stripes on a pseudosection, data points having a high information content of resistivity change within the reservoir would occur along diagonals centered at station 11 and particularly at  $n$ -spacings of 5, 6, and 7. The dipole-dipole electrode array was used in this study because it is sensitive to lateral discontinuities in subsurface resistivity, even when these occur beneath a conductive overburden layer (Beyer, 1977).

It may be observed in Figure 1 how resistivity changes have evolved with time and how by the Fall 1981, 2.5 years after the baseline data set was collected, a definite resistivity increase developed along the western part of the reservoir region, and a broad resistivity decrease developed along the eastern margin of the reservoir.

Near-surface resistivities are seen to be increasing on both ends of the line. The increase on the west (stations 1 through 6) is believed due to an increased level of irrigation. The increase on the east may be related to increased underflow of Colorado River waters because of high runoff last year.

#### SIMULATION OF A RESERVOIR WITH TWO WATERS OF DIFFERENT SALINITY

To simulate the resistivity changes we begin by considering production of liquid water from a porous  $\alpha$  reservoir with an initial temperature of  $T = 300^\circ\text{C}$ . The vertical pressure profile is assumed hydrostatic, with an average pressure  $P_{\text{av}} = 120$  bars. The reservoir communicates with recharge waters of  $T = 100^\circ\text{C}$  above and at the margins. The mass fraction of recharge water is denoted by  $x$ ; initially  $x = 0$  in the reservoir. The recharge waters are assumed to have different (lower) salinity than the water initially in place in the reservoir. For purposes of numerical modeling, however, we ignore all differences in thermophysical properties arising from different salinity, such as differences in viscosity, density, boiling curve, etc. We write separate mass balances for "water 1" ( $x = 0$ ) and "water 2" ( $x = 1$ ), which makes it possible to keep track of the individual waters as they start flowing and mixing in response to production. A similar approach was presented by Geshelin et al. (1981) for tracing fluid migration during steam assisted oil recovery.

The reservoir simulations were carried out with LBL's compositional simulator MULKOM, which is similar to the geothermal reservoir simulator SHAFT79 (Pruess and Schroeder, 1980), except

that two water components are included. In this paper we will describe only one of the models for which calculations were made. Other results were previously presented by Pruess et al. (1982). The model shown in Figure 2 is a two-dimensional reservoir with recharge from above (vertical recharge) and the sides (horizontal recharge); the bottom is assumed to be an impermeable boundary. The vertical recharge zone begins 600 m beneath the surface and extends to the reservoir top at 800 m depth. The vertical extent of the reservoir is 400 m and its lateral width is 1600 m.

Due to symmetry, only one half of the system needs to be modeled. Laterally, the reservoir is connected to a recharge zone of 1000 m length with boundary conditions of  $T = 100^\circ\text{C}$ ,  $x = 1$  on the outer boundary. The initial distributions in temperature and fluid composition between reservoir and vertical and lateral recharge boundaries are assumed to vary smoothly as follows:

(i) composition:

$$x_{\text{in}} = \begin{cases} 0 & \text{in reservoir;} \\ f(\ell) & \text{between reservoir and} \\ & \text{recharge boundary;} \\ 1 & \text{at recharge boundary;} \end{cases}$$

(ii) temperature:

$$T_{\text{in}} = \begin{cases} 300^\circ\text{C} & \text{in reservoir;} \\ 300 - f(\ell) \times (300-100)^\circ\text{C} & \text{between reservoir and} \\ & \text{recharge boundary;} \\ 100^\circ\text{C} & \text{at recharge boundary.} \end{cases}$$

Here  $\ell$  is the distance from the vertical or horizontal reservoir boundary, and

$$f(\ell) = \begin{cases} \frac{2}{L^2} \ell^2 & \text{for } \ell < L/2 \\ 1 - \frac{2}{L^2} (\ell-L)^2 & \text{for } \ell > L/2, \end{cases}$$

$L$  is the vertical or horizontal distance between reservoir and recharge boundaries ( $L_{\text{vertical}} = 200$  m;  $L_{\text{horizontal}} = 1000$  m).

The computational mesh employs 100 m horizontal and 50 m vertical spacing, for a total of  $(18 \times 8) + (8 \times 4) = 176$  elements, plus elements for representing the boundaries. The problem is initialized with approximate gravitational equilibrium relative to a reference pressure of  $p = 120$  bars at 1000 m depth. (Due to the temperature differences between reservoir and recharge waters no rigorous gravitational equilibrium is possible). Production rate was taken as 600 kg/s ( $\sim 2,160$  tonnes/hr), approximately the actual average production rate at Cerro Prieto. Fluid sources of equal size are

placed in elements D1, E3, D5, and E7 of the model (Figure 2).

Horizontal permeability is taken to be  $100 \times 10^{-15} \text{ m}^2$ , corresponding to a  $kH = 40 \times 10^{-12} \text{ m}^3$ . This agrees closely with the "field value"  $36 \times 10^{-12} \text{ m}^3$ , which can be derived from an average transmissivity  $kH/\mu = 0.4 \times 10^{-6} \text{ m}^3/\text{Pa.s}$  (Liguori, 1979) and  $\mu (300^\circ\text{C}) = 9.01 \times 10^{-5} \text{ Pa.s}$ . Vertical permeability was assumed one tenth of horizontal permeability. For these permeabilities, the reservoir can easily sustain the applied production rate. The largest observed pressure decline after 5 years is approximately 1 MPa, so that pressures remain well above saturation pressure and no two-phase zones evolve.

Temperature profiles for layers C, E, and G after 3 years of simulation are presented in Figure 3. The initial temperature distribution ( $t = 0$ ) is also plotted for comparison. The figure shows a significant cooling in the lateral recharge zone (850 to 1600 m from the line of symmetry) due to the massive exploitation. Lateral migration of the recharge waters is evident in Figure 3 from a comparison of temperature profiles for layers C and G to the initial temperature distribution ( $t = 0$ ). The temperatures in layer G are everywhere higher than the temperatures in layers C and E in the outside region ( $> 800 \text{ m}$  away from the symmetry line) because of buoyancy effects. The migration of the colder recharge waters from above is evident from the lower temperatures in the G layer in comparison with the temperature profile in the C layer in the production region.

The composition profiles for layers C, E, and G after 3 years of simulation are shown in Figure 4. Again, the initial composition profile ( $t = 0$ ) is included for reference. The compositional change within the reservoir and lateral recharge zones, as well as buoyancy effects, are clearly evident and are more pronounced than the temperature changes. Compositional change within the production region is dominated by vertical recharge. Accordingly, the mass fraction of recharge water is greatest in layer G, and smallest in layer C near the bottom of the reservoir. A different picture is observed at the reservoir margins at a distance of 800 m from the symmetry line. There lateral recharge is dominant, which, due to buoyancy effects, tends to be stronger in the lower portions of the reservoir, so that  $x$  (layer C)  $> x$  (layer E)  $> x$  (layer G). The buoyancy effects cause  $x$  (layer G) to decrease more rapidly away from the lateral recharge boundary (at 1800 m distance from the symmetry line) than is observed for layer E or C. Notice that in layer G vertical recharge causes minimum in  $x$  near the reservoir margin (800 m). A complex interplay of vertical and lateral recharge is also observed for layer E.

#### RESISTIVITY MODELING OF A RESERVOIR WITH WATER MIXING

A two-dimensional finite difference computer code was used in numerical calculations for resistivity models in this study. The code RESIS2D solves finite difference equations for the electric potentials in or on the surface of a two-dimensional half space with an arbitrary conductivity distribution (Dey and Morrison, 1976; Dey, 1976).

The code utilizes a mesh of  $113 \times 16$  nodes of which  $58 \times 13$  can be used for arbitrary resistivity distributions. Because of the limited mesh size, only 32 elements were used to describe resistivity within the production zone, and thus resistivity variations due to temperature and salinity changes were averaged over fairly large cross-sectional areas. This should produce some inaccuracies but these are not considered significant for the purposes of this demonstration. A larger source of error lies in the fact that we use a simple, schematic reservoir model as the sole basis for creating an initial subsurface resistivity distribution. This distribution, described in the next section, is different from the one developed by Wilt and Goldstein (1981a) from the field data. As a result, the percent changes in calculated resistivity from the baseline resistivities will contain an error that is a function of the volume averaged difference between model and true subsurface resistivities.

#### CALCULATION OF RESISTIVITY VARIATIONS

A study of the variations in resistivity due to changes in fluid properties in geothermal systems has recently been published (Ershagi et al., 1981). In the present paper we use those results to calculate resistivity as a function of salinity and temperature.

Figure 5 indicates the effect of salinity and temperature on resistivity for "typical" sediments in a geothermal environment. For our study we assume that recharge waters have .3% dissolved solids by weight and are at a temperature of  $100^\circ\text{C}$ . In the production zone the parameters are 1.5% and  $300^\circ\text{C}$ , respectively. These values are based on observed water chemistry at Cerro Prieto (Grant et al., 1981). Figure 5 shows that resistivity variations due to salinity and temperature changes can be quite large. In the recharge zone, initial resistivity is 50 percent larger than in the production zone due to temperature variation and more than 300 percent larger due to salinity differences.

The initial subsurface resistivity distribution assumed in this study is shown in Figure 6. The 5 ohm-m surface layer corresponds to a cap-rock. The 15.6 ohm-m background is sedimentary rock with 15 percent porosity and saturated

with 100°C water at .3 weight percent NaCl. The 15.6 ohm-m resistivity value for the background was calculated from Archie's law. The geothermal reservoir is represented by a 1600 m x 400 m zone buried at a depth of 800 m. Within the reservoir region the resistivity is initially 2.15 ohm-m. This number was derived by adjusting the background of 15.6 ohm-m for increased salinity and temperature in the reservoir region. Note that the center of the model (Station 6) would correspond to Station 11 in the field data (Figure 1).

#### RESULTS AND DISCUSSION

Resistivity calculations for the two-dimensional resistivity model were made for a dipole-dipole array centered over the reservoir. In the calculations a dipole length of 800 m was used because of convenience, rather than 1000 m as used in the field survey. Therefore, calculated and field results are not geometrically identical but the differences should not deter simple comparisons. Resistivity pseudosections were calculated for various points in the production history; prior to production and then at times of 0.5, 1, 3, and 5 years after the onset of production. Apparent resistivity changes for each time relative to preproduction are then calculated and presented in pseudosection form in Figure 7.

Despite the large rate of production the apparent resistivity changes are small after one year of production. During such early times, production - related resistivity changes might be obscured by seasonal variations in rainfall, runoff, or irrigation or obscured by measurement errors if sufficient accuracy cannot be achieved (Wilt and Goldstein, 1982). However, it is clear from this example that the hydraulic (salinity) front moves relatively rapidly, and that significant changes in apparent resistivity appear between one and three years after the start of production.

A comparison of the simulated resistivity changes to the actual changes for times of 1, 1.5, and 2.5 years after the 1979 baseline data (Figure 1) reveals that the field data show a far more complex pattern of change, but there are also similarities in pattern and magnitude that deserve mention. Notice that only the western limb of the resistivity increase emerges after 2.5 years (Fall 1981). The asymmetry in the resistivity change indicates an asymmetry in the physical processes, in distinction from the symmetrical recharge of our schematic model. There is no unique solution to the problem, but a fluid flow model that might produce the observed changes is one proposed by Halfman et al. (1982); i.e., (a) cooler, less saline recharge from the west and above, and (b) hot, saline recharge from below and from the east.

Second, because the initial resistivity model is not an accurate facsimile of what we believe

the true resistivity distribution was in 1979, there is little chance that the model results would match the observed field changes. That they match as well as they do in places, suggests that we are on the right track toward understanding the reservoir processes.

#### CONCLUSIONS

A methodology has been presented for indirect study of a geothermal reservoir which combines numerical reservoir simulation with modeling of apparent resistivities as measured with the dipole-dipole technique. For a Cerro Prieto-type reservoir, temporal changes in apparent resistivity due to production and recharge of colder and less saline waters are both calculated and are observed to be substantial over time intervals of several years. It therefore appears feasible to use resistivity for monitoring reservoir processes. Our schematic models predict resistivity changes which are only approximately comparable to field observations, and thus more refined numerical models will be required.

For most geothermal reservoirs, the patterns of fluid flow and resistivity change will be three-dimensional. Therefore, accurate resistivity monitoring requires measurements along several intersecting profiles.

The proposed methodology should also be applicable for monitoring the migration of reinjected fluids.

#### ACKNOWLEDGEMENT

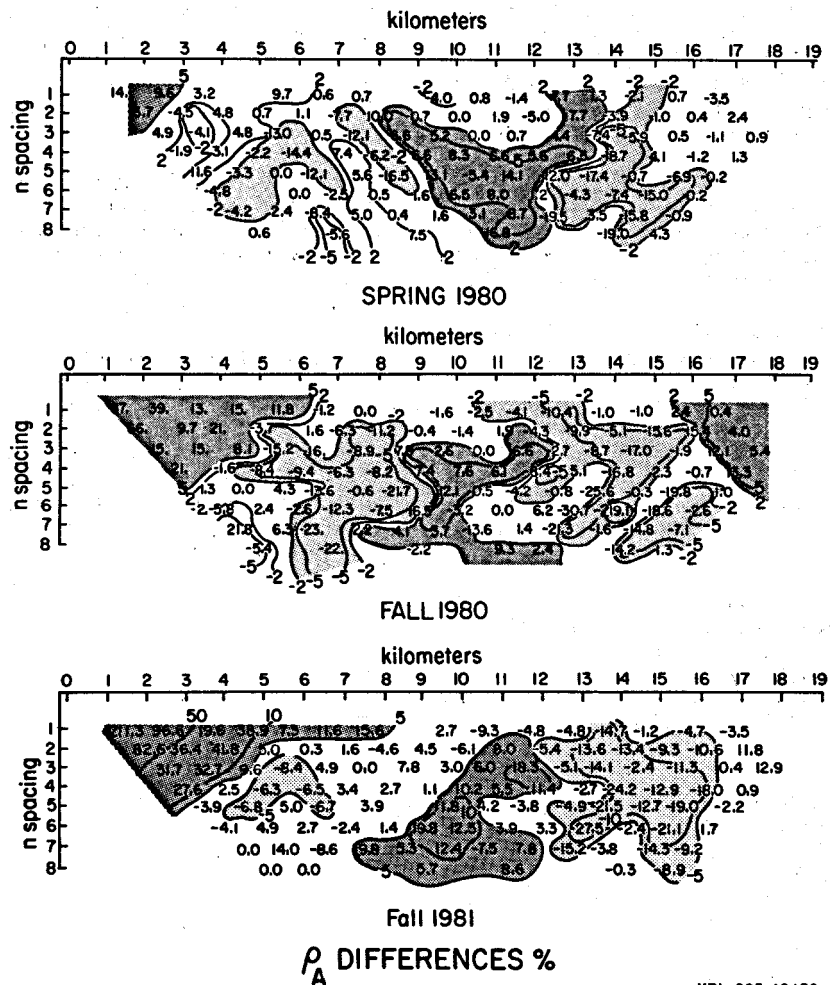
We thank Drs. M. Lippmann and C.F. Tsang for a critical review of the manuscript. This work was supported by the Assistant Secretary for Conservation and Renewable Energy, Office of Renewable Technology, Division of Geothermal and Hydropower Technologies of the U.S. Department of Energy under Contract No. DE-AC03-76SF00098.

TABLE 1  
Parameters for Production Simulation

|                         |  |
|-------------------------|--|
| rock density            | 2600 kg/m <sup>3</sup>                 |
| porosity                | 15%                                    |
| horizontal permeability | $100 \times 10^{-15} \text{ m}^2$      |
| vertical permeability   | $10 \times 10^{-15} \text{ m}^2$       |
| heat conductivity       | 2.1 W/m°C                              |
| rock specific heat      | 900 J/kg°C                             |
| vertical extent         |  |
| of reservoir            | 400 m                                  |
| volumetric rate         |  |
| of production           | $9.74 \times 10^{-7} \text{ kg/s.m}^3$ |
| initial reservoir       |  |
| temperature             | 300°C                                  |
| average initial         |  |
| reservoir pressure      | 12 MPa (120 bars)                      |

REFERENCES

- Bartel, L.C., and Wayland, J.R. (1981), "Results from Using the CSAMT Geophysical Technique to Map Oil Recovery Processes," Paper SPE 10230, presented at the 56th Annual Fall Technical Conference and Exhibition of the SPE, San Antonio, Texas, October 5-7, 1981.
- Beyer, J.H. (1977), "Telluric and D.C. Resistivity Techniques Applied to the Geophysical Investigation of Basin and Range Geothermal Systems, Part II: A Numerical Model Study of the Dipole-Dipole and Schlumberger Resistivity Methods," Lawrence Berkeley Laboratory, Report LBL-6325 2/3.
- Dey, A. (1976), "Resistivity Modeling for Arbitrarily Shaped Two Dimensional Structures, Part II: Guide to the FORTRAN Algorithm RESIS2D," Lawrence Berkeley Laboratory Report LBL-5283.
- Dey, A., and Morrison, H.F. (1976), "Resistivity Modeling for Arbitrarily Shaped Two-Dimensional Structures, Part I: Theoretical Formulation," Lawrence Berkeley Laboratory Report LBL-5233.
- Ershaghi, I., Dougherty, E.E., and Hardy, L. (1981), "Formation Evaluation in Liquid Dominated Geothermal Reservoirs," Report for Department of Energy No. DOE/ET/28384-T1.
- Geshelin, B.M., Grabowski, J.W., and Pease, E.C. (1981), "Numerical Study of Transport of Injected and Reservoir Water in Fractured Reservoirs During Steam Stimulation," Paper SPE 10322, presented at 56th Annual Fall Technical Conference and Exhibition of the SPE, San Antonio, Texas, October 5-7, 1981.
- Grant, M.A., Truesdell, A.H., and A. Mañón M. (1981), "Production induced Boiling and Cold Water Entry in the Cerro Prieto Geothermal Reservoir Indicated by Chemical and Physical Measurements," In Proceedings, Third Symposium on the Cerro Prieto Geothermal Field, Baja California, Mexico, Lawrence Berkeley Laboratory Report LBL-11967, pp 221-237.
- Halfman, S.E., Lippmann, M.J., Zelwer, R., and Howard, J.H. (1982), "Fluid Flow Model of the Cerro Prieto Geothermal Field Based on Well Log Interpretation," Lawrence Berkeley Laboratory, LBL-14898, 13 p.
- Liguori, P.E. (1979), "Simulation of the Cerro Prieto Geothermal Field Using a Mathematical Model," In Proceedings, Second Symposium on the Cerro Prieto Geothermal Field, Mexicali, Baja California, October 17-19, 1979, p. 521-524.
- Pruess, K., and Schroeder, R.C. (1980), "SHAFT79 User's Manual," Lawrence Berkeley Laboratory Report LBL-10861, Berkeley, California.
- Risk, G.F. (1975), "Monitoring the Boundary of the Broadland Geothermal Field, New Zealand," Proceedings, Second United Nations Symposium on the Development and Use of Geothermal Resources, San Francisco, California, May 20-29, 1975, v. 2, p. 1185-1189.
- Wilt, M.J., and Goldstein, N.E. (1981a), "Resistivity Monitoring at Cerro Prieto," Geothermics, v. 10, n. 3/4, p. 183-194.
- Wilt, M.J., and Goldstein, N.E. (1981b), "Results from Two Years of Resistivity Monitoring at Cerro Prieto," In Proceedings, Third Symposium on the Cerro Prieto Geothermal Field, Baja California, Mexico, Lawrence Berkeley Laboratory Report LBL-11967, p. 372-379.
- Wilt, M.J., and Goldstein, N.E. (1982), "Interpretation of Dipole-Dipole Resistivity Monitoring Data at Cerro Prieto," In Proceedings, Fourth Symposium on the Cerro Prieto Geothermal Field, Guadalajara, Mexico, August 10-12, 1982, in preparation.



XBL 825-10150

Figure 1. Resistivity pseudosections measured over the Cerro Prieto Geothermal Field shown as percent changes from the 1979 baseline data set.

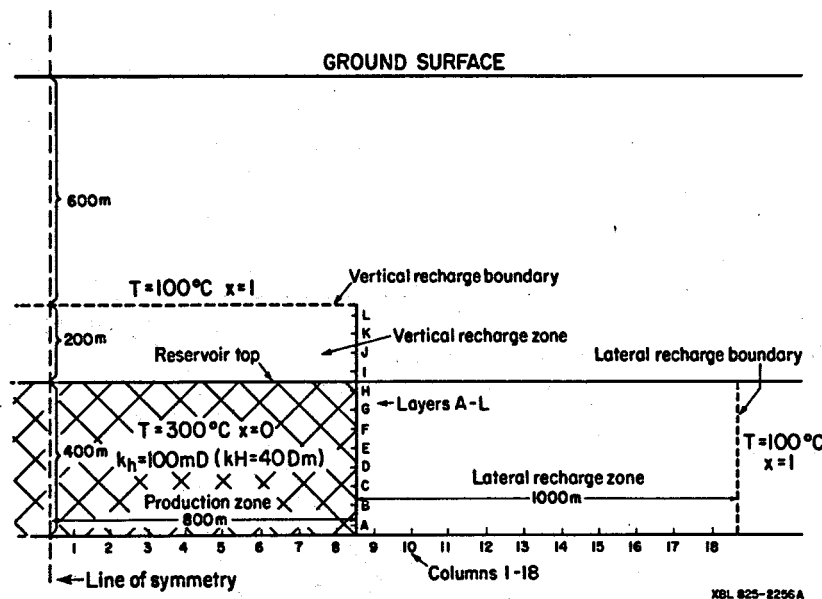


Figure 2. Two-dimensional reservoir model for vertical and lateral recharge.

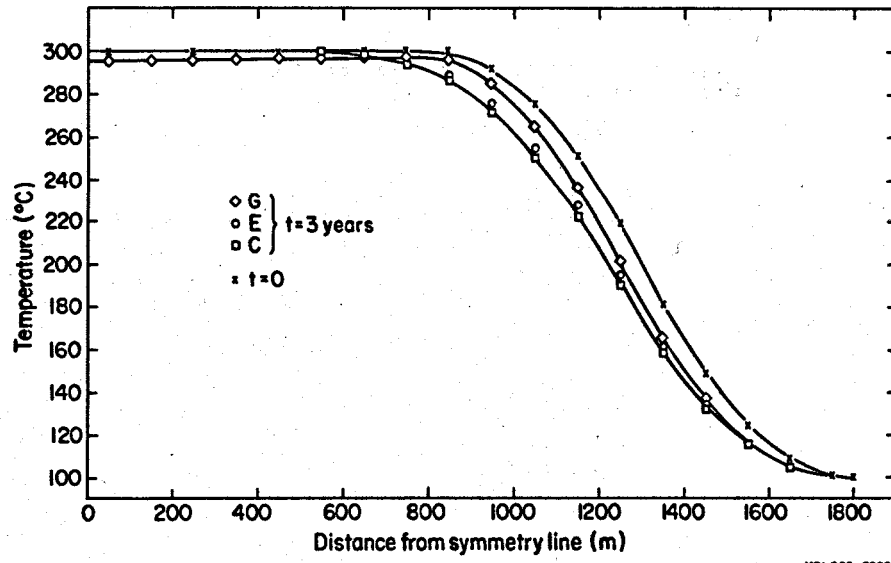
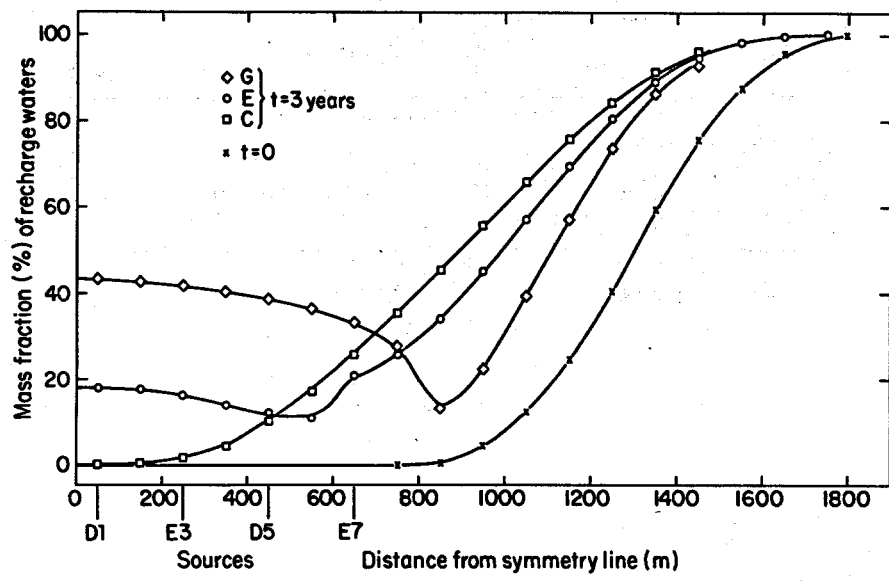


Figure 3. Temperature profiles for two-dimensional model.



XBL825-2254

Figure 4. Composition profiles for two-dimensional model.

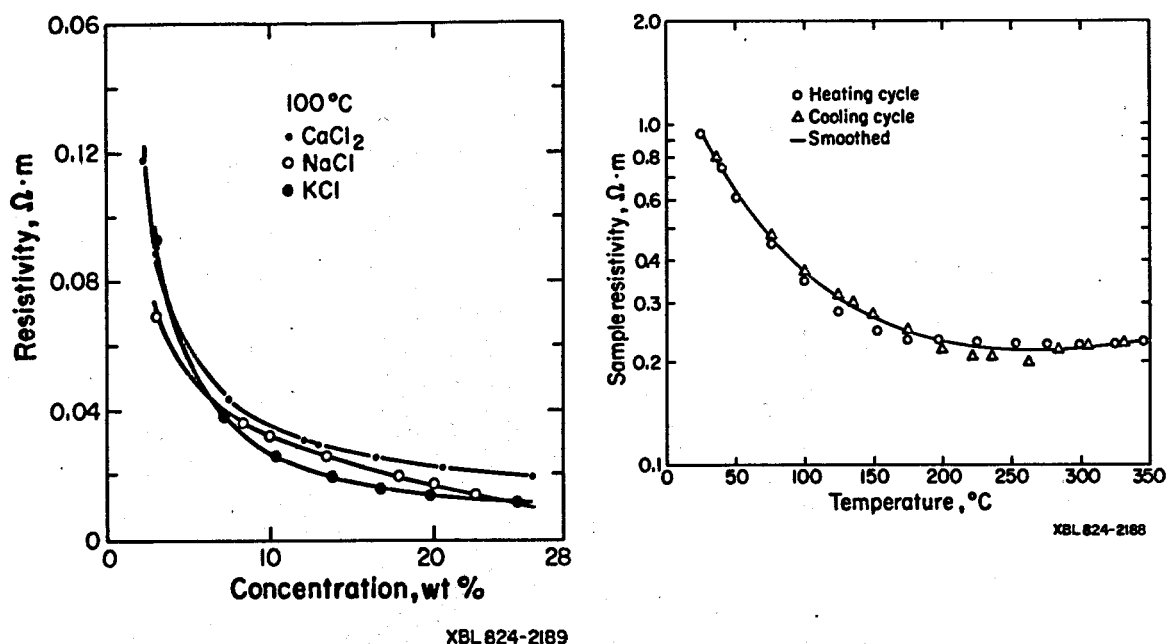


Figure 5. Dependence of resistivity on (a) salinity and (b) temperature for sedimentary rocks.

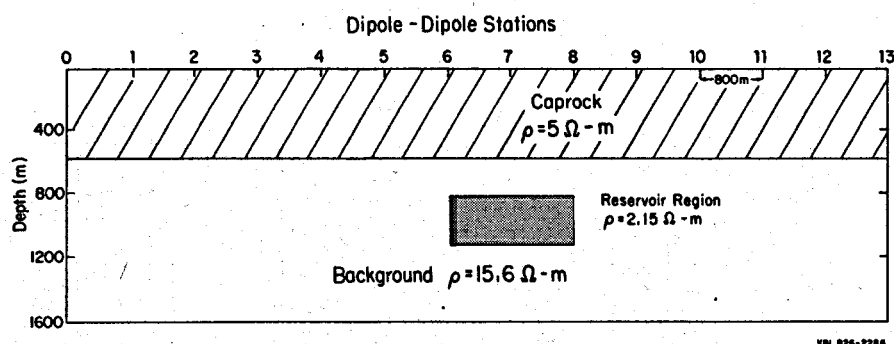
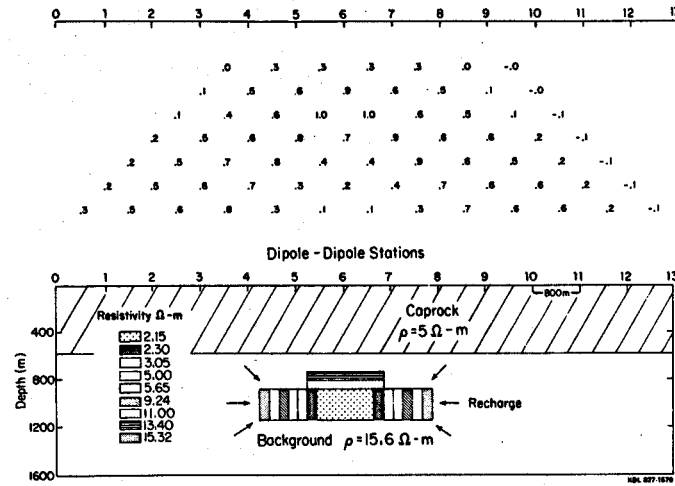
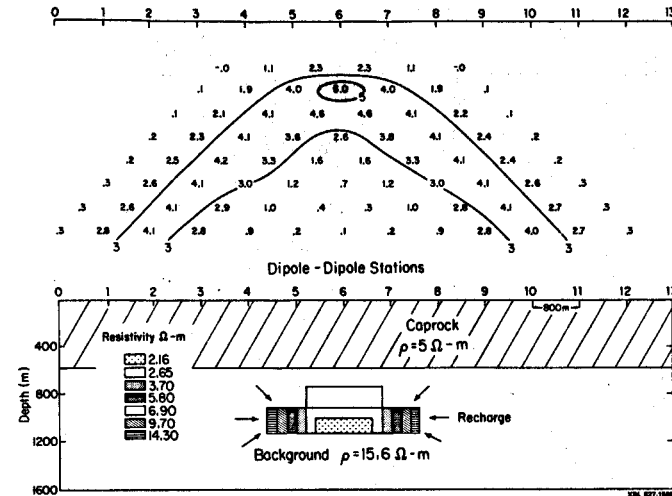


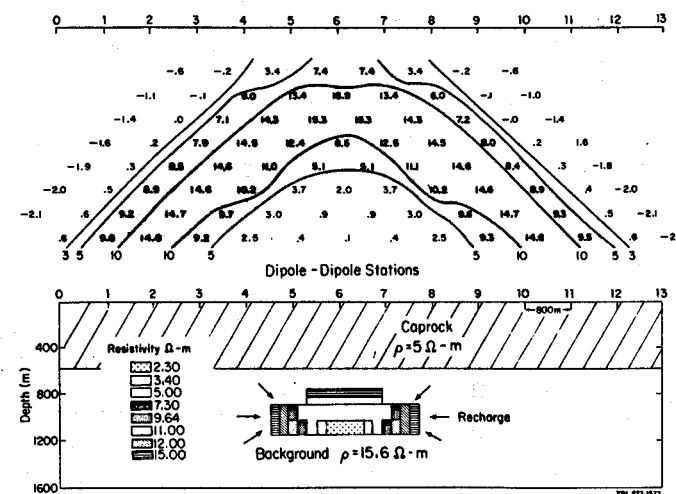
Figure 6. Undisturbed resistivity distribution.



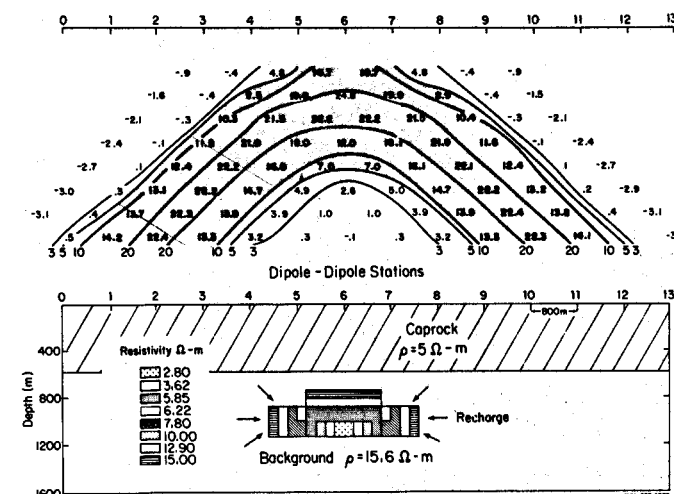
(A)



(B)



(C)



(D)

Figure 7. Resistivity pseudosections for reservoir with vertical and lateral recharge (percent changes) at (A) Six months, (B) One year, (C) Three years, and (D) Five years after the beginning of production at rate of 600 kg/s.